

THE GLOBAL PRECIPITATION MEASUREMENT (GPM) MISSION FOR SCIENCE AND SOCIETY

GAIL SKOFRONICK-JACKSON, WALTER A. PETERSEN, WESLEY BERG, CHRIS KIDD, ERICH F. STOCKER, DALIA B. KIRSCHBAUM, RAMESH KAKAR, SCOTT A. BRAUN, GEORGE J. HUFFMAN, TOSHIO IGUCHI, PIERRE E. KIRSTETTER, CHRISTIAN KUMMEROW, ROBERT MENEGHINI, RIKO OKI, WILLIAM S. OLSON, YUKARI N. TAKAYABU, KINJI FURUKAWA, AND THOMAS WILHEIT

The GPM mission collects essential rain and snow data for scientific studies and societal benefit.

Water is essential to our planet. It literally moves mountains through erosion, transports heat in Earth's oceans and atmosphere, keeps our planet from freezing as a result of radiative impacts of atmospheric water vapor, and causes catastrophes through droughts, floods, landslides, blizzards, and severe storms, but most importantly water is vital for nourishing all life on Earth. Precipitation as a source of freshwater links Earth's water and energy cycles. Thus, knowing when, where, and how precipitation falls is of paramount importance for science and society.

While there are areas of the world that have dense ground-based sensors for measuring precipitation in the form of rain gauges and radars, the vast oceans, less populated regions, and parts of developing countries lack adequate surface measurements of precipitation (Kidd et al. 2017). Satellites provide an optimal platform from which to measure precipitation globally. In 1997, NASA and the National Space Development Agency of Japan (NASDA), now known as the Japan Aerospace Exploration Agency (JAXA; see the appendix for a list of key acronyms and abbreviations used in this paper), launched the Tropical

AFFILIATIONS: SKOFRONICK-JACKSON, STOCKER, KIRSCHBAUM, BRAUN, HUFFMAN, AND MENEGHINI—NASA Goddard Space Flight Center, Greenbelt, Maryland; PETERSEN—NASA Marshall Space Flight Center, National Space Science and Technology Center, Huntsville, Alabama; BERG AND KUMMEROW—Colorado State University, Fort Collins, Colorado; KIDD—University of Maryland, College Park, College Park, Maryland; KAKAR—NASA Headquarters, Washington, D.C.; IGUCHI—National Institute of Information and Communications Technology (NICT), Tokyo, Japan; KIRSTETTER—NOAA/National Severe Storms Laboratory, Norman, Oklahoma; OKI AND FURUKAWA—Japan Aerospace Exploration Agency, Tokyo, Japan; OLSON—Joint Center for Earth Systems Technology, University of Maryland, Baltimore

County, Baltimore, Maryland; TAKAYABU—University of Tokyo, Tokyo, Japan; WILHEIT—Texas A&M University, College Station, Texas

CORRESPONDING AUTHOR: Gail Skofronick-Jackson, gail.s.jackson@nasa.gov

The abstract for this article can be found in this issue, following the table of contents.

DOI:10.1175/BAMS-D-15-00306.1

In final form 25 November 2016

©2017 American Meteorological Society

For information regarding reuse of this content and general copyright information, consult the [AMS Copyright Policy](#).

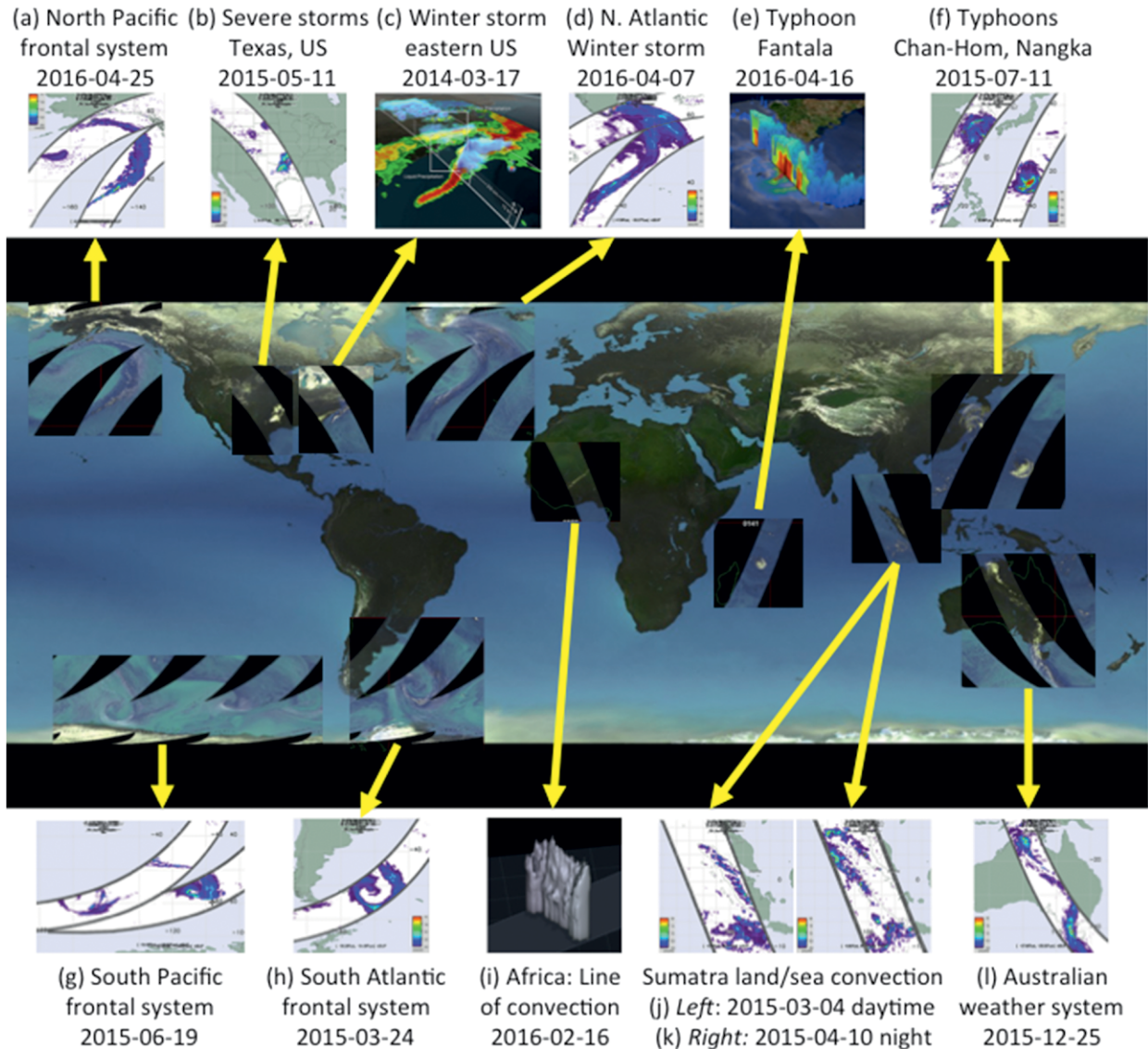


FIG. 1. GPM CO GMI composite BT and example precipitation event cases. (middle) Composite 89-GHz brightness temperatures averaged over 24 months showing the latitudinal extent of the GPM CO measurements. Example precipitation cases include (a) a North Pacific frontal system from GMI, (b) severe storms in TX from GMI, (c) a winter storm over the eastern United States as observed in 3D from the DPR, (d) a North Atlantic winter storm from GMI, (e) Typhoon Fantala as observed in 3D from the DPR, (f) Typhoons Chan-Hom and Nangka in two successive orbits from GMI, (g) a South Pacific frontal system from GMI, (h) a South Atlantic frontal system from GMI, (i) a line of convection in Africa in 3D from the DPR, Sumatra land–sea convection during the (j) day and (k) night from GMI, and (l) an Australian weather system from GMI.

Rainfall Measuring Mission (TRMM; Simpson et al. 1988; Kummerow et al. 1998, 2000), which operated until April 2015. The TRMM spacecraft had both a passive microwave multifrequency imaging radiometer (provided by NASA) and a Ku-band radar channel (provided by NASDA) capable of generating three-dimensional views of precipitation structure (Kozu et al. 2001). TRMM's data continue to foster important scientific investigations, such as those by Curtis et al. (2007), Adler et al. (2009), Shepherd et al.

(2011), Liu et al. (2012), Houze et al. (2015), and Liu and Zipser (2015). In addition, TRMM has a large user community that has applied these data operationally to support decision-making (Kirschbaum et al. 2017).

The Global Precipitation Measurement (GPM) Core Observatory (GPM CO) spacecraft is an advanced successor to TRMM, with additional channels on both the dual-frequency precipitation radar (DPR) and on the GPM Microwave Imager (GMI) with capabilities to sense light rain and falling snow (Hou

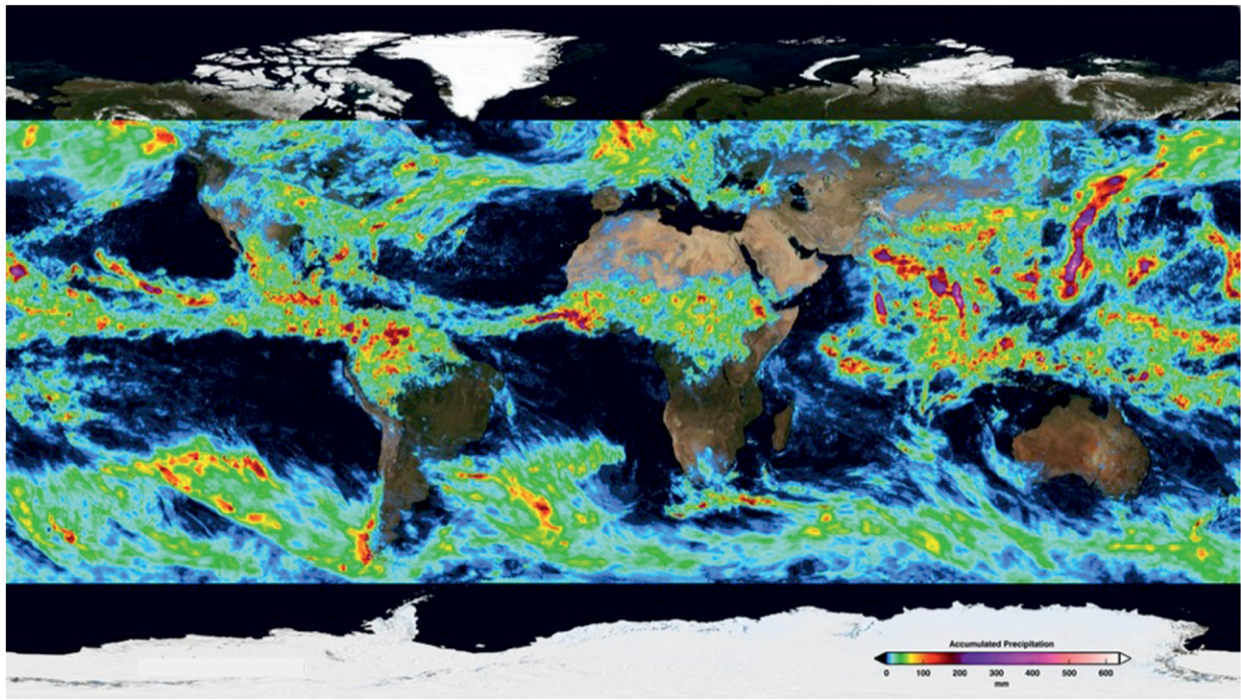


FIG. 2. IMERG accumulated precipitation totals from 4 to 11 Aug 2014. The IMERG retrieval algorithm has not yet been developed for pole-to-pole retrievals. The large accumulation near Japan is Typhoon Halong. The accumulation also shows a major storm over the North Sea near Europe, the origins of Hurricane Gonzalo on the western coast of Africa, and a deep tropical depression that produced floods across northern India. IMERG gridded products are produced every 30 min with $0.1^\circ \times 0.1^\circ$ grid boxes, currently covering the latitude band 60°N – 60°S .

et al. 2008, 2014). The GPM CO, also a NASA–JAXA partnership, was launched in February 2014 and currently operates in a non-sun-synchronous orbit with an inclination angle of 65° . This orbit allows the GPM CO to sample precipitation across all hours of the day from the tropics to the Arctic and Antarctic circles and for observing hurricanes and typhoons as they transition from the tropics to the midlatitudes. GPM expands TRMM's reach not only in terms of global coverage, but also through sophisticated satellite instrumentation, the intercalibration of datasets from other microwave radiometers, coordinated merged precipitation datasets, reduced latency for delivering data products, simplified data access, expanded global ground-validation efforts, and integrated user applications. Because of the application focus of GPM, the public release of precipitation products is required in near-real time (1–5 h after the observations are downlinked to the ground stations).

The GPM mission has several scientific objectives, including 1) advancing precipitation measurements from space; 2) improving knowledge of precipitation systems, water cycle variability, and freshwater availability; 3) improving climate modeling and prediction capabilities; 4) improving weather forecasting and four-dimensional (4D) reanalysis; and 5) improving

hydrological modeling and prediction. More details about these scientific objectives can be found in Hou et al. (2014).

GPM CO's well-calibrated instruments allow for scientifically advanced observations of precipitation in the midlatitudes, where a majority of Earth's population lives. The middle panel in Fig. 1 shows the coverage of the GPM CO, and several interesting precipitation events are shown in Figs. 1a–l. These examples indicate the breadth of GPM's observational capabilities through measurements of diverse weather systems, such as severe convection, falling snow, light rain, and frontal systems over both land and ocean. The measurements include surface precipitation rates available from GMI and three-dimensional precipitation structure from DPR.

A founding concept of the GPM mission is the constellation of precipitation observations provided by national and international satellite partners of opportunity. International and national partnerships are formed independently by both NASA and JAXA for sharing satellite data, ground validation measurements, and scientific expertise (Hou et al. 2014). The GPM CO serves as a calibrator to ensure unified precipitation estimates from all satellite partners at high temporal (0.5–3.0 h) and spatial (5–15 km) scales

GPM'S MISSION SCIENCE REQUIREMENTS

Prior to the GPM's launch in 2014, NASA formally documented Core Observatory requirements to be met within GPM's 3-year prime mission operations period in order for GPM to be deemed fully successful. Several of these requirements dealt with instrument performance or operational elements (e.g., orbit maintained to within ± 1 km of operational orbital attitude) and will not be discussed here. Most of the requirements pertained to scientific accuracy and science data and are key to ensuring stable and validated precipitation products expected by both scientific investigators and application users. Specifically, these science requirements include the following:

- Measurements of the same geophysical scenes using both active and passive techniques from 65°N to 65°S with mean sampling time of 24 h.
- Using the DPR,
 - quantify rain rates between 0.22 and 110.00 mm h^{-1} and
 - detect snowfall at an effective resolution of 5 km.
- Using the GMI,
 - quantify rain rates between 0.2 and 60.0 mm h^{-1} and
 - detect snowfall at an effective resolution of 15 km.
- Estimate the precipitation particle size distribution (e.g., quantitative estimates of precipitation microphysical properties such as the mean median mass diameter of the particle size distribution to within $\pm 0.5 \text{ mm}$).
- Provide calibrated ground-based precipitation measurements and associated error characterizations at 50-km horizontal resolution for comparison with space-based radar and radiometer measurements at designated ground validation sites within ground tracks of the GPM *Core Observatory*.
 - The biases in instantaneous rain rates between the ground-based and space-based estimates should not exceed 50% at 1 mm h^{-1} or 25% at 10 mm h^{-1} .
 - The random errors between the ground-based and space-based estimates should not exceed 50% at 1 mm h^{-1} or 25% at 10 mm h^{-1} .
- To provide data in near-real time for hurricane monitoring, numerical weather prediction, hydrological model forecasts, and other application and operational uses,
 - combined radar–radiometer swath products will be available within 3 h of observation time, 90% of the time, and
 - radiometer precipitation products will be available within 1 h of observation time 90% of the time.

All science requirements have been met and are currently being documented in peer-reviewed literature. Selected publications can be found in the AMS featured collection on GPM (<http://journals.ametsoc.org/topic/gpm>).

(Hou et al. 2014). Such satellite precipitation datasets can be merged via algorithms and accumulated over time, as shown in Fig. 2. These GPM products allow for detailed investigations of how and where precipitation is distributed and how these patterns change over days, seasons, and years. These estimates are also used to model and estimate hazard impacts (e.g., floods and droughts), weather-related disasters, agricultural forecasting, and famine warnings (Kirschbaum et al. 2017).

The GPM CO instruments and constellation concept will be discussed in the next section. Then, precipitation retrieval algorithms, data products, processing, and availability will be presented. The fourth

section will be devoted to early validation results. In the conclusions section, the paper will summarize how GPM data have been used over the past 2 years for selected scientific investigations and societal applications. Material presented herein has been gathered primarily from the U.S. Science Team. Nevertheless, it is important to note that the current and future successes of GPM are a joint effort with our international partners, especially Japan. The paper will close with conclusions and next steps.

GPM CORE OBSERVATORY AND CONSTELLATION CONFIGURATION.

An essential activity of the GPM mission is the use of the NASA–JAXA GPM CO to unify and intercalibrate datasets generated by constellation satellite partners and merge these into next-generation, high temporal resolution global precipitation estimates. Fundamental to the success of this activity is both the GPM CO instrumentation and the constellation configuration.

GPM Core Observatory. GPM CO was launched at 0337 Japan standard time (JST) 28 February 2014 (1837 UTC 27 February 2014) from Tanegashima Island, Japan. The prime mission lifetime (instrument design life) is 3 years and 2 months (for checkout), but fuel is projected to last well beyond that, potentially lasting 15 or more years if the instruments/spacecraft systems (e.g., batteries) do not fail and fuel requirements do not increase. The GMI and DPR together provide a powerful synergistic tool to assess precipitation micro- and macrostructures, intensity, and phase globally at relatively high (regional) resolutions. The DPR with Ku-band (35.5 GHz) and Ka-band

(13.6 GHz) channels provides three-dimensional precipitation (rain and snow) particle structure with vertical resolution of 250 m, a horizontal resolution of ~5 km, and swath widths of 125 (Ka) and 245 km (Ku) (Hou et al. 2014). The DPR was extensively calibrated prelaunch (Kojima et al. 2012) and its performance meets mission requirements (e.g., Kubota et al. 2014, 2016; Toyoshima et al. 2015). (See also the sidebar on GPM's mission science requirements.)

The GMI is a 13-channel conically scanning microwave radiometer [see Table 1 and Hou et al. (2014) for details]. GMI provides wide-swath (885 km) brightness temperatures (T_B) data to estimate surface precipitation at resolutions ranging from 5 to 25 km depending on frequency. Design requirements for GMI were driven both by requirements to build a priori databases to support Bayesian microwave precipitation retrieval algorithms (Kummerow et al. 2011, 2015), as well as to provide a reference radiance calibration standard for the GPM constellation (Hou et al. 2014). The design features needed to meet the requirements include a shroud over the warm load to eliminate solar intrusions, a robust reflective antenna coating to minimize emissivity issues, and the addition of noise diodes for a four-point calibration of the window channels (Draper et al. 2013, 2015a,b).

The GMI instrument is meeting its performance requirements (Draper et al. 2015a,b) and has already been deemed to be one of the best-calibrated conically scanning passive microwave radiometers in space, with brightness temperature accuracy levels for all channels within 0.4 K and stability within 0.2 K (Wentz and Draper 2016).

GPM constellation configuration. The GPM mission encompasses the GPM CO and a constellation of about 10 satellites (as of May 2017) from national and international partners of opportunity [see Table 1 and Hou et al. (2014) for details]. These satellites are designed and operated for the partners' missions, but these agencies are willing to share their data with GPM for the purpose of producing next-generation unified global precipitation estimates. The constellation satellites bearing passive radiometers fly independent polar or non-sun-synchronous orbits allowing for multiple coincident overpasses with the GPM CO.

For the constellation partner data, the first step toward unified precipitation estimates is the intercalibration of T_B using GMI as the reference standard. This ensures that the observed T_B are consistent among the sensors with expected differences after accounting for variations in the observing

TABLE 1. Channel availability by frequency and polarization (V indicates vertically polarized, H indicates horizontally polarized) for the GPM constellation radiometers. GMI, TMI, AMSR2, and SSMIS are all conically scanning imagers while MHS, ATMS, and SAPHIR are cross-track-scanning water vapor sounders. ATMS is currently operating on board *Suomi-NPP* with a second copy to launch on board JPSS-1 in late 2017.

Sensor	Satellite	6–7 GHz	10 GHz	18–19 GHz	21–23 GHz	31–37 GHz	85–92 GHz	150–166 GHz	183 GHz
GMI	GPM	—	10.65 (V, H)	18.7 (V, H)	23.8 (V)	36.64 (V, H)	89.0 (V, H)	166 (V, H)	183.31 (V) \pm 3, \pm 7
TMI	TRMM	—	10.65 (V, H)	19.35 (V, H)	21.3 (V)	37.0 (V, H)	85.5 (V, H)	—	—
AMSR2	GCOM-WI	6.925 (V, H), 7.3 (V, H)	10.65 (V, H)	18.7 (V, H)	23.8 (V, H)	36.5 (V, H)	89.0 (V, H)	—	—
SSMIS	DMSP F16, F17, F18, F19	—	—	19.35 (V, H)	22.235 (V)	37.0 (V, H)	91.655 (V, H)	150 (H)	183.31 (H) \pm 1, \pm 3, \pm 6.6
MHS	NOAA-18, NOAA-19, MetOp-A, MetOp-B	—	—	—	—	—	89 (V)	157 (V)	183.31 (H) \pm 1, \pm 3, 190.31 (V)
ATMS	Suomi NPP, JPSS-1	—	—	—	23.8 (V)	31.4 (V)	88.2 (V)	165.5 (H)	183.31 (H) \pm 1, \pm 1.8, \pm 3, \pm 4.5, \pm 7
SAPHIR	Megha-Tropiques	—	—	—	—	—	—	—	183.31 (H) \pm 0.2, \pm 1.1, \pm 2.8, \pm 4.2, \pm 6.8, \pm 11

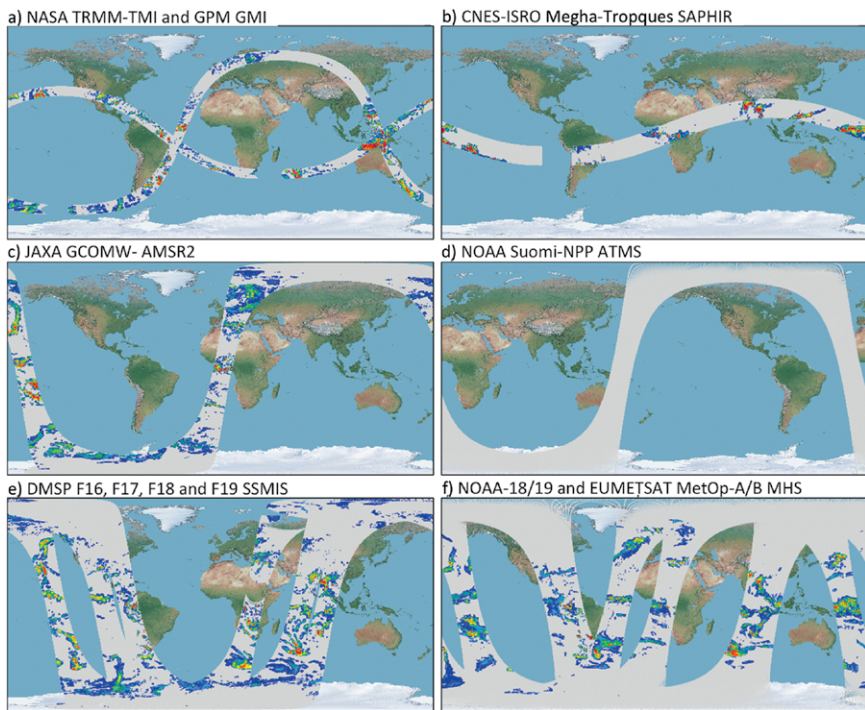


FIG. 3. Precipitation estimates are shown for a single orbit of each of the GPM constellation radiometer types for 1 Jan 2015. (left) The conically scanning window-channel radiometers and (right) the cross-track scanning water vapor sounding radiometers are shown. The constellation radiometers include (a) TMI and GMI on board the NASA TRMM and GPM satellites, (b) SAPHIR on board the CNES-ISRO Megha-Tropiques satellite, (c) AMSR2 on board JAXA's GCOM-WI satellite, (d) ATMS on board NOAA's Suomi NPP satellite, (e) SSMIS on board the DMSP F16, F17, F18, and F19 satellites, and (f) MHS on board the NOAA-18, NOAA-19, and EUMETSAT MetOp-A and MetOp-B satellites.

frequencies, bandwidths, polarizations, and view angles (Wilheit 2013, 2015; Zavodsky et al. 2013; Zhang et al. 2011, 2016; Table 1). Figure 3 shows the extent of coverage provided by single 98-min orbits for each of the various radiometer types in the GPM constellation.

Sensor intercalibration between GMI and the partner sensors involves several steps, as described in Wilheit (2013), Wilheit et al. (2015), and Berg et al. (2016). Multiple independent approaches are compared during these steps, which help to identify flaws or limitations of a given approach, thus increasing confidence in the results and providing a measure of the uncertainty in the resulting calibration adjustments. After adjustments, residual differences between GMI channels and those on the constellation radiometers are generally smaller than 1 K (Berg et al. 2016). This is a remarkable achievement that now allows the project to focus on the precipitation products rather than T_B uncertainties.

Future satellite intercalibration tasks include understanding and quantifying the residual uncertainties

in the estimated calibration differences due to the radiative transfer models and geophysical parameter retrievals and adapting to changes in the radiometer constellation. Updates in the GMI calibration algorithms and subsequent intercalibration adjustments to the constellation sensors will occur during scheduled reprocessing of retrieval products. In addition, intercalibrating TRMM's TMI and pre-GPM microwave constellation sensor data to GMI is necessary for generating a consistent long-term next-generation precipitation record that covers the TRMM and GPM eras.

ALGORITHMS, DATA PRODUCTS, DATA PROCESSING, AND DATA AVAILABILITY.

The GPM CO data processing is a joint NASA-JAXA effort. NASA data processing is done at GSFC

(Greenbelt, Maryland) in the Precipitation Processing System (PPS). JAXA data processing is carried out at the Tsukuba Space Center (Tsukuba, Ibaraki, Japan) in the Mission Operations System (MOS). The interconnected architecture of this joint mission ground system can be seen in Fig. 4. Working with the GPM principal investigators and science algorithm developers, PPS maintains the operational science data processing system and ensures the timely processing of all GPM science instrument data [see Hou et al. (2014) for a table of GPM products]. During routine operations, raw instrument data (level 0 data) are received in near-real time by the PPS and processed using science algorithms to produce calibrated, swath-level instrument [level 1 (L1)] data. JAXA's MOC processes DPR level 1 products along with their level 3 merged satellite products. Additional algorithms are used to compute geophysical parameters such as precipitation rate at the swath-level resolution (level 2, L2 data products). [For reference, a special collection of papers describing the L2 precipitation algorithms is appearing in the

Journal of Atmospheric and Oceanic Technology; see the Precipitation Retrieval Algorithms for GPM featured collection online (<http://journals.ametsoc.org/topic/gpm>).] At the final stage of processing, level 3 (L3) algorithms produce gridded and accumulated geophysical parameters including products such as latent heating profiles (e.g., Tao et al. 2016). It is envisioned that level 4 data products developed through model-assimilated precipitation forecasts and analyses will be available in the future.

The GPM mission has both near-real-time (NRT) and research-quality production requirements. Both NASA and JAXA contribute key processing efforts to fulfill these latency requirements. The NRT products are generated by using forecasts or earlier forms of ancillary data.

NRT products include GMI T_B , and precipitation estimates from GMI (denoted GPROF), DPR, and the combined radar–radiometer algorithm (CORRA; Kummerow et al. 2015; Seto et al. 2015; Grecu et al. 2016). GMI products are available within an hour of data collection while DPR and CORRA results are available within 3 h of data collection. Another NRT product developed by the U.S. team is the Integrated Multisatellite Retrievals for GPM

(IMERG) gridded retrieval, which is a level 3 NASA product (Huffman et al. 2015). JAXA produces an analogous product called Global Satellite Mapping of Precipitation (GSMap; Kubota et al. 2007; Aonashi et al. 2009; Ushio et al. 2009). IMERG uses GPM-CO to intercalibrate precipitation data from all constellation radiometers. Temporal and spatial gaps in the IMERG microwave precipitation estimates (e.g., as shown in Fig. 3) are filled by morphing the estimates in between the microwave overpasses and incorporating IR estimates with a Kalman filter where the gaps are too long (over about 3 h) to produce $0.1^\circ \times 0.1^\circ$ half-hour global products. The IMERG product is produced twice in NRT: once approximately 5 h after data collection and again approximately 14 h after data collection.

All of the NRT products are also processed as research products. The geolocation of the research products is more consistent as predictive ephemeris rarely needs to be used. Research products are produced by PPS when all the required high-quality ancillary and geolocation data are received with the objective for accuracy, completeness, and consistency. These research products are available hours to months after data collection and are stable for long-term precipitation

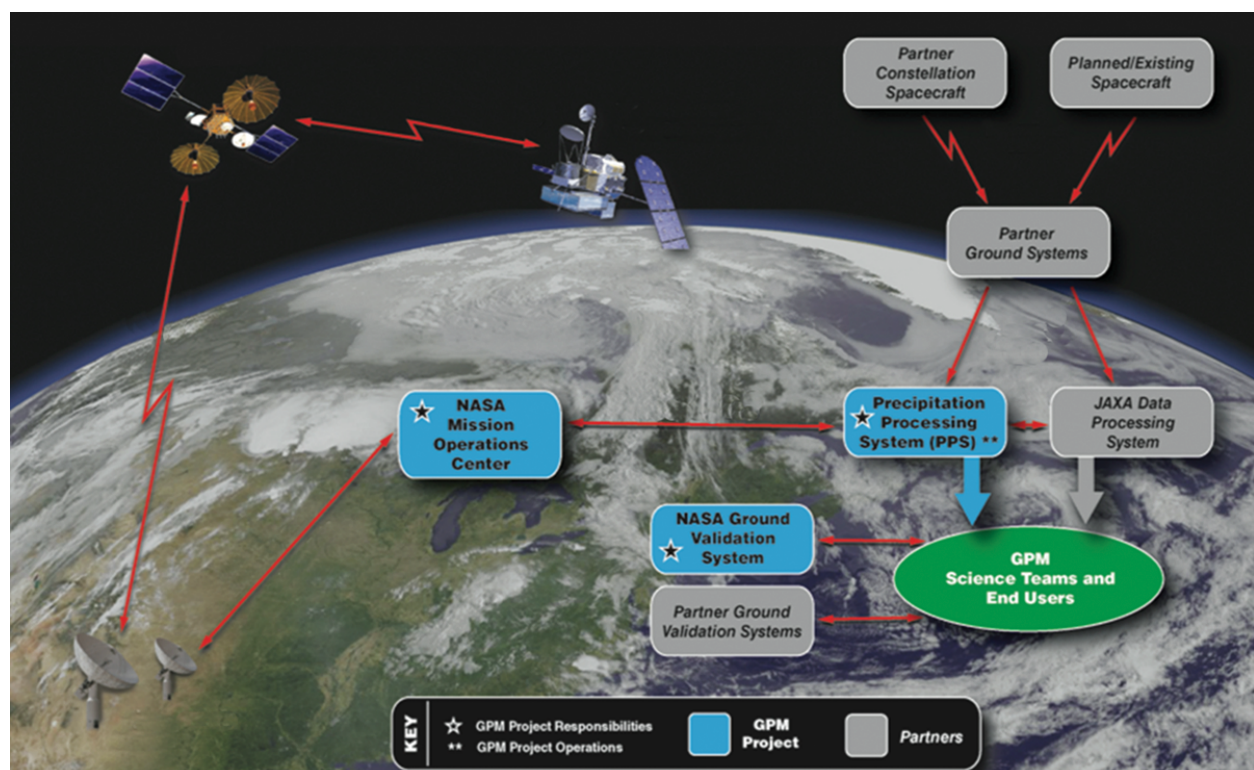


FIG. 4. GPM mission operations data and communication system. GPM CO satellite data are downlinked in near-real time via the NASA Tracking and Data Relay Satellite System (TDRSS) to White Sands, NM, where the GPM Mission Operations Center retrieves it, ensures its integrity, and passes it to PPS. Partner data, ancillary information, and validation measurements are also processed by mission operations.

investigations. PPS generates and distributes all data from the instruments on the core satellite as well as level 2 and level 3 data from the partner constellation satellites. In addition to the standard HDF5 format files, a Geographic Information System (GIS; TIFF world files) product and ASCII text files are provided for selected product estimates. All GPM data are openly available and accessible online (<https://pmm.nasa.gov/data-access/downloads/gpm>). JAXA's GPM products in general can also be obtained online (www.gportal.jaxa.jp/gp/top.html), as can the GSMAp multisatellite merged dataset (<http://sharaku.eorc.jaxa.jp/>). GPM data (level 0–3) are periodically reprocessed as retrieval algorithms are improved. The at-launch [version 03 (V03)] IMERG products were biased high for heavy rain events, while the upgrades to V04 (March 2017) and to V05 (planned for mid-2017) progressively reduced this bias. GPM retrieval algorithms use the dual-frequency channels of DPR and the high-frequency channels of GMI and hence precipitation products from GPM are different than those from TRMM. Nevertheless, there are plans to reprocess intercalibrated precipitation data (in winter 2017/18) to produce

a consistent long-term precipitation record that starts at the beginning of the TRMM era. GPM is meeting data latency requirements (as shown in the sidebar), on average, greater than 99% of the time. Recent PPS statistics show nearly 50 TB of data are downloaded by more than 1,000 unique users from all over the world in a single month.

VALIDATION EFFORTS. GPM Ground Validation (GV) efforts include the direct statistical validation and verification of satellite estimates against high-quality ground measurements and physical validation for algorithm improvement and hydrological models. Validating data are garnered from both regular ongoing surface observations and focused field campaigns (Hou et al. 2014; see also <https://pmm.nasa.gov/index.php?q=science/ground-validation>). Major GPM validation efforts include 1) comparisons among satellite precipitation products, 2) comparisons against ground datasets, and 3) analyses for meeting mission requirements.

One evaluation technique compares the zonal means among the various GPM instrument algorithms and

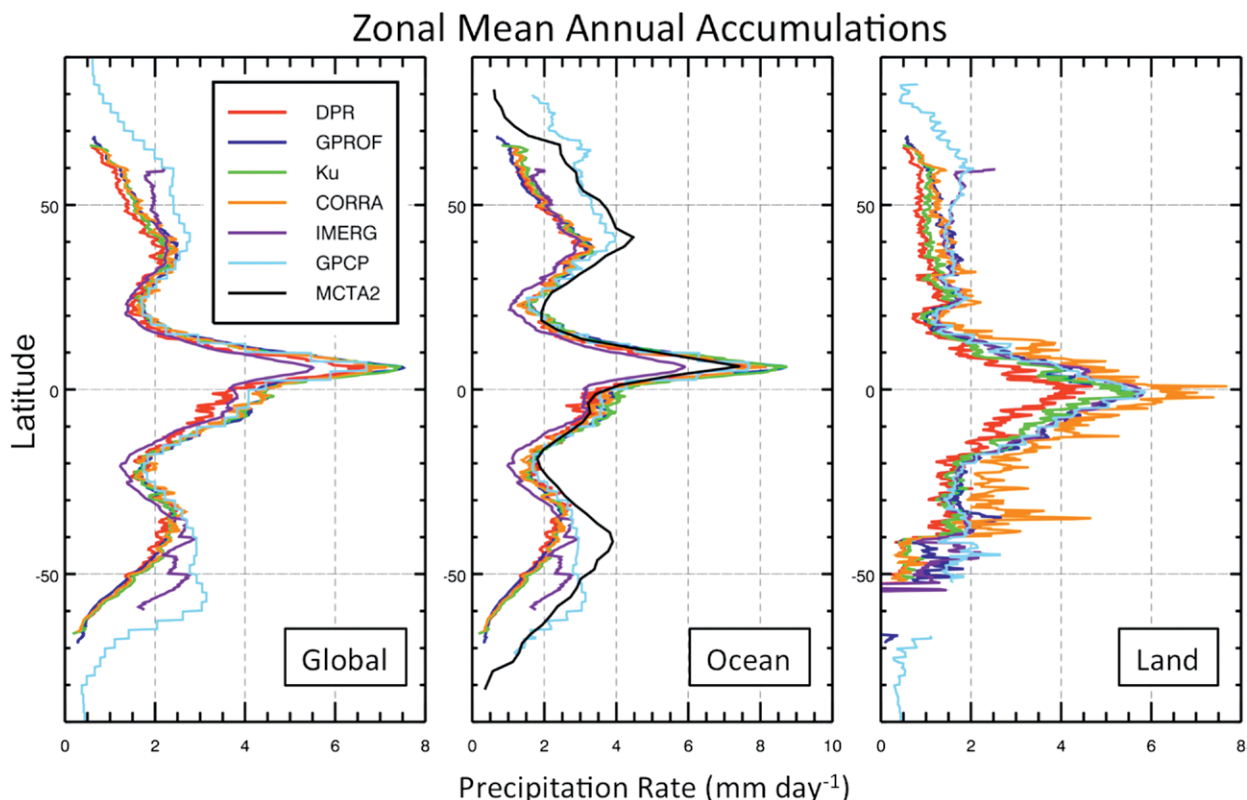


FIG. 5. Zonal precipitation averages (mm day^{-1}) for the full annual cycle during 2015. The five estimates are GPM DPR (dual-frequency radar; red), GPM GPROF (GMI passive radiometer; blue), GPM Ku band (single-frequency radar; green), GPM CORRA (DPR + GMI; orange), IMERG (GPM merged with constellation estimates; purple), GPCP global estimates (light blue), and MCTA2 estimates over ocean (black, covering the years 2007–10). The GPCP is version 2.3, MCTA is version 2, IMERG is version 03, and the other GPM products are version 04.

established precipitation estimates such as the Global Precipitation Climatology Project (GPCP) datasets (Adler et al. 2003) and, over ocean, the Merged *Cloud-Sat*, TRMM, and *Aqua* version 2 (MCTA2) dataset (Behrangi et al. 2014). Both GPCP and MCTA2 include a variety of input datasets selected for their utility in precipitation estimation at both low and high latitudes. We show the global zonal means for 2015 for land and ocean (Fig. 5a), ocean only (Fig. 5b), and land only (Fig. 5c). Figure 5 illustrates that DPR, Ku-band, CORRA, and GPROF algorithm retrievals are in good agreement. The GPM zonal accumulations underestimate with respect to the MCTA at higher latitudes. This is most attributable to the fact that the DPR minimum detectable reflectivities correspond to minimum rain rates of approximately 0.2 mm h^{-1} . Since much of the higher-latitude precipitation is light, and CORRA and GPROF are based on DPR estimates, GPM is low in the higher latitudes. A high-latitude, light-precipitation solution for GPROF was implemented in the version 05 algorithm release. The mean daily precipitation (mm day^{-1}) for each of the algorithms is provided in Table 2, which shows that IMERG's annual precipitation is lower than the other algorithms while there are interesting differences among the diverse approaches over land. Land surfaces tend to complicate the retrieval process and the various algorithms use different approaches to mitigate surface (emissivity and clutter) issues.

Direct statistical GV of GPM rainfall-rate estimates relies primarily on existing high-resolution, quality-controlled U.S. national radar network rain-rate products such as the NOAA/National Severe Storms Laboratory–University of Oklahoma Multi-Radar/Multi-Sensor (MRMS) products (e.g., Zhang et al. 2016, and references therein). Currently, the MRMS system (<http://mrms.ou.edu>) incorporates data from all polarimetric WSR-88Ds (NEXRAD), a large number of automated rain gauge networks, and model analyses in the continental United States (CONUS) and southern Canada. The system creates a gridded mosaic of quantitative precipitation estimate (QPE) products on a $0.01^\circ \times 0.01^\circ$ grid at a 2-min temporal resolution [see Zhang et al. (2016) for the most recent updates]. Of particular value to

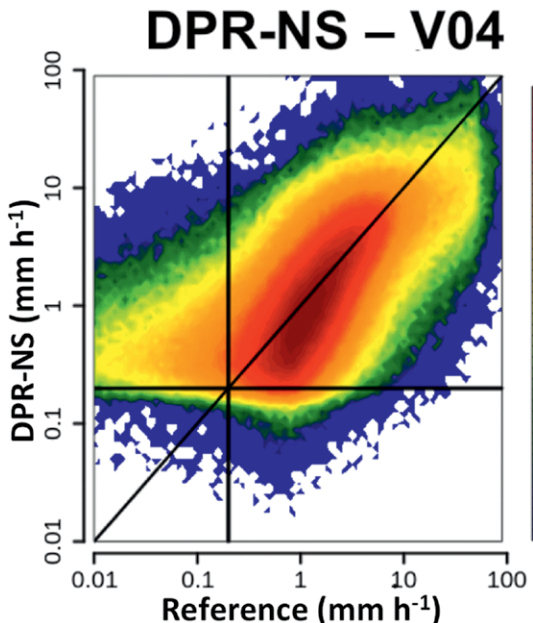
TABLE 2. Area-weighted mean annual precipitation (mm day^{-1}) for each of the algorithms globally, over land, and over ocean from 50°N to 50°S latitude. The GPCP is version 2.3, IMERG is version 03, and the other GPM products are version 04.

	Global-mean daily precipitation	Oceanic-mean daily precipitation	Land-mean daily precipitation
DPR	2.51	2.77	1.72
GPROF	2.86	2.99	2.36
Ku band	2.81	3.03	2.05
CORRA	2.83	2.85	2.77
IMERG	2.48	2.44	2.39
GPCP	2.95	3.15	2.43
GSMaP	2.74	2.83	2.12

GPM GV are MRMS radar-based gauge-adjusted QPEs. Collectively, these MRMS products provide an independent and consistent reference for directly evaluating postlaunch GPM precipitation products across a large number of meteorological regimes as a function of resolution, accuracy, and sample size (Kirstetter et al. 2012).

For continental-scale verification of GPM products over the CONUS, all MRMS data coincident with GPM orbits are continuously processed and saved as a GPM GV dataset (<http://wallops-prf.gsfc.nasa.gov/NMQ/index.html>). In addition to standard MRMS quality control procedures (see Zhang et al. 2016), additional procedures for minimizing radar uncertainties are employed to derive a high-quality precipitation reference at the satellite product pixel resolution (Kirstetter et al. 2012). Filtering out instances when the radar–gauge ratios are outside of the range 0.1–10.0 further refines the instantaneous gauge bias-corrected MRMS product. In addition, only radar data with the best measurement conditions (i.e., no beam blockage and radar beam below the melting layer) defined by a radar quality index (RQI) are retained. Gridded 0.01° MRMS products can then be matched to allow direct comparisons between the surface radar and satellite precipitation products (see Fig. 6).

Independent comparisons of this GPM GV MRMS reference dataset with two dense, well-maintained, and data quality-controlled NASA rain gauge networks show that for a $\sim 5\text{-km}$ footprint with 30-min accumulations of $>0.5 \text{ mm h}^{-1}$, biases are $<10\%$ while normalized mean absolute errors (NMAE) are $<35\%-40\%$. These results are consistent with a quantitative assessment of the MRMS accuracy performed at its native resolution (Kirstetter et al. 2015a). Individual satellite radar matches are subsequently averaged to



◀ FIG. 6. Density scatterplot of DPR-NS V04 vs reference MRMS precipitation (mm h^{-1}) at the footprint scale over the period Jun 2014–Aug 2015. The 1:1 line (solid diagonal line) is displayed as well as the detection limit for the DPR (0.22 mm h^{-1}). The data shown focus on the conditional case of the satellite footprint and reference-mean precipitation rates both being nonzero ($>0.01 \text{ mm h}^{-1}$) and a precipitation type of liquid only.

sampling times (e.g., coincident swath and MRMS sample time) as a density scatterplot for individual near-surface DPR sensor footprint scales (effective resolution of 5 km). Here, it is important to note that the scatter of the data exhibited in Fig. 6 is expected based on the instantaneous nature of the comparison at high spatial resolution (e.g., effective FOV) and the related intrinsic random error associated with matching the associated precipitation estimates in time and space between MRMS and GPM L2 data swaths. Comparisons at this scale are best interpreted as a tool for evaluating the broader systematic bias behavior between GPM products using the GV as a third reference.

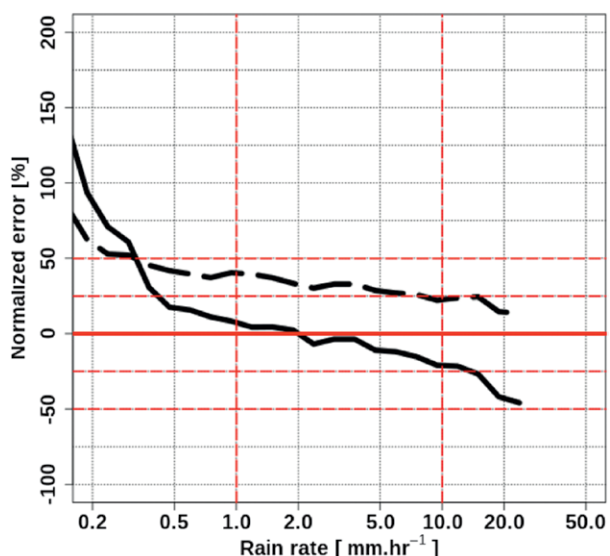
In Fig. 6, good agreement between the GV MRMS reference and the near-surface DPR normal scan (NS) algorithm, version 04, is evident with a bias [defined as the mean relative error (MRE)] and a normalized mean absolute error (NMAE) of only -9.8% and 51.7% , respectively. The normal scan mode of DPR consists of retrievals using the Ku-band 245-km-wide-swath data. The agreement is particularly good for rain rates in the $1.0\text{--}10.0 \text{ mm h}^{-1}$ range. Note that the minimum detectable signal of the DPR ($\sim 0.2 \text{ mm h}^{-1}$, in terms of rainfall) and partial beam filling are responsible for scatterplot differences at very low rain rates. Contingency statistics for DPR NS rain detection reveal that ground “reference” rain rates $>0.2 \text{ mm h}^{-1}$ (the lower requirement

coarser 50-km grids, which are useful for quick-look comparison products (cf. <http://wallops-prf.gsfc.nasa.gov/NMQ/index.html>) and for verifying GPM level 1 science requirements (e.g., Fig. 7). Here, the increased spatial averaging of the footprints together with the removal of outliers (5th and 95th percentiles) maintains a low bias while further reducing the random error in the MRMS data relative to the 5-km-footprint scale mentioned above.

The GPM GV MRMS reference dataset and its derivatives have revealed and quantified several aspects of satellite-estimated rainfall retrieval errors and uncertainties including comparisons of rainfall detectability and rainfall-rate distributions (Kirstetter et al. 2014), separation of systematic biases and random errors (Kirstetter et al. 2012), regional precipitation biases (Chen et al. 2013), the influence of precipitation subpixel variability and surface (Kirstetter et al. 2015b; Carr et al. 2015), and comparisons between satellite products (Kirstetter et al. 2013, 2014; Tan et al. 2016, 2017).

Figure 6 provides an example of comparisons to GPM core satellite products for instantaneous

► FIG. 7. Conditional DPR V04 bias (MRE; solid black) and random error (mean absolute error; dashed black) vs the MRMS reference precipitation rate (mm h^{-1}) at 50-km resolution over the period Jun 2014–Aug 2015 and normalized by the bin-mean rain rate. Points falling outside of the 5%–95% interquartile range (outliers) were not included in this comparison. The dashed red lines indicate that the GPM mission science requirements reached 50% (25%) at the specified precipitation rates of 1.0 (10.0) mm h^{-1} .



threshold specified for DPR rain detection based on radar sensitivity) yield a DPR probability of detection (POD) of 64%, a false-alarm rate of 9%, and a Heidke skill score (HSS) of 37%.

GPM mission science requirements (see sidebar) stipulate thresholds for detection, bias, and random error (Hou et al. 2013). For example, rain-rate estimates should exhibit a bias and random error of $\leq 50\%$ (25%) at rain rates of 1 (10) mm h^{-1} for areas of $50 \text{ km} \times 50 \text{ km}$. Figure 7 is presented for the DPR NS product as a preliminary example of assessing bias and random error. For nonzero raining pixels in Fig. 7, the bias in each reference rain bin is computed as the MRE in percent while for the random error the NMAE is computed with the systematic error (bias) removed. Figure 7 suggests that the above GPM mission science requirements have been met for the DPR example shown and the method used. While these results

are encouraging, work is ongoing to further test and refine methodologies for determining product-consistent lower rain-rate thresholds for comparing GPM GPROF, CORRA, DPR, and MRMS datasets and for defining error types, as well as to meet the other GPM mission science requirements.

INITIAL SCIENTIFIC INVESTIGATIONS AND APPLICATIONS. With 2 years' worth of calibrated and validated precipitation estimates, GPM's data are being used for scientific studies (e.g., Liu and Liu 2016; Wentz and Meissner 2016; Panegrossi et al. 2016; Prakash et al. 2016). Most of the science results are from investigations by members of the NASA Precipitation Measurement Missions (PMM) science team (in 2016 consisting of 60 principal investigators from NASA centers and U.S. universities funded by NASA Headquarters while the Japanese PMM science team consists of 41 principal investigators). NOAA

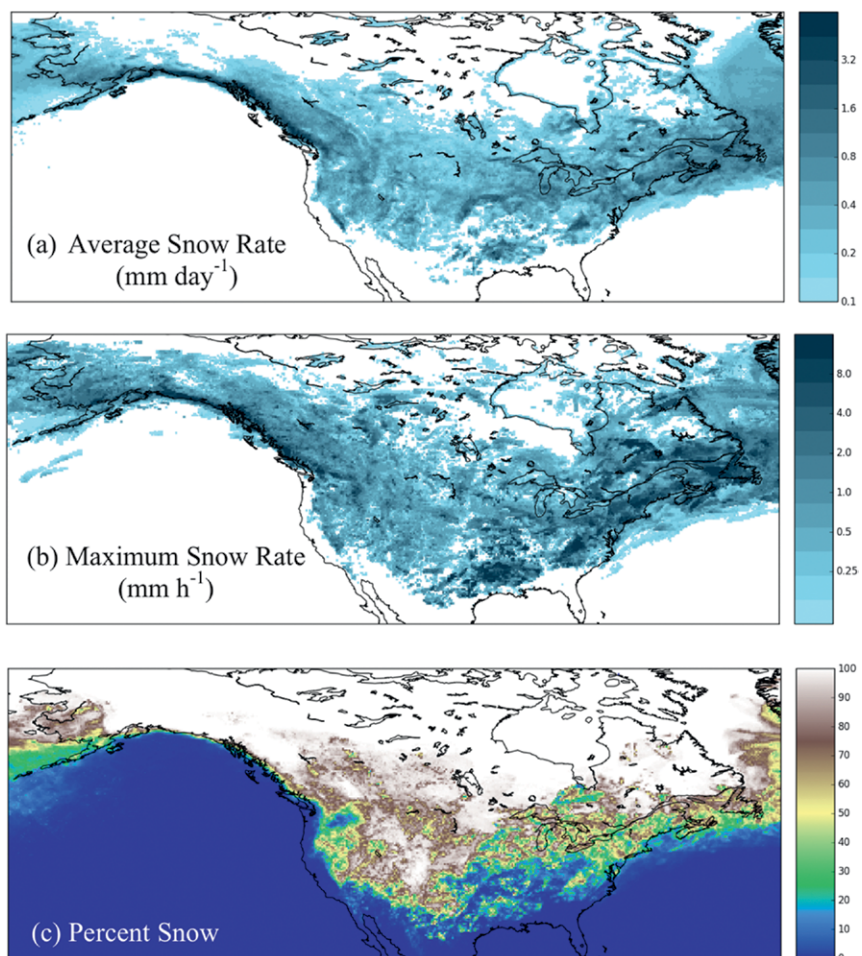


FIG. 8. (a) Average and (b) maximum liquid equivalent snowfall rates and (c) the fraction of precipitation that was identified as falling snow (and not liquid rain) from Dec 2014 to Feb 2015 from the GMI GPROF (V04) retrieval algorithm.

has a team of 16 investigators involved with GPM and more than 20 international no-cost teams also play important roles in GPM science and validation efforts. Herein, two scientific investigations are reported upon: falling snow retrievals and monsoon studies.

Scientifically, retrievals of falling snow from space represent an important dataset for understanding Earth's atmospheric, hydrological, and energy cycles. While satellite-based remote sensing provides global coverage of falling snow events, the science is relatively new and retrievals are still undergoing development addressing challenges such as those listed in Skofronick-Jackson et al. (2015). GPM's mission goal of estimating falling snow is demonstrated in an example from 17 March 2014, just 18 days after launch (Fig. 1c). More generally, the GMI observed the average snow rate, maximum snow rate, and fraction of precipitation that fell as snow over the winter of 2014/15 (Fig. 8). While these snow estimates are

not fully validated, they do support the requirement that GPM detect falling snow. The high rates over the south-central states may not be representative of typical winter conditions but may have resulted from the occurrence of several heavy snow events in mid- to late February of 2015 when GMI had good overpasses. Of particular note for this period were the large snowfall rates along the western coast of Canada and the southern coast of Alaska, where coastal topography may enhance local snowfall rates.

Looking elsewhere, the GPM mission can track the advance and retreat of India's annual monsoon and the tropical storms that impact India's population. As shown in Fig. 9, GPM observes the detailed structure of the copious monsoon precipitation as it marches from south to north across India over the seasons, with Tropical Cyclone Hudhud (October 2014) on the left and storm Roamu (May 2016) on the far right of the timeline. Figure 9 shows the advance of the monsoon from offshore in May to inland by July and the retreat back to the Bay of Bengal from September to November over 2 years' of GPM data. Over longer precipitation records, interannual variations due to the effect of large-scale oceanic or atmospheric patterns or to climate change may be identified, information that is crucial for societal applications and benefits.

Integrating satellite observations into land surface modeling systems is a critical component of resolving the state of the water cycle and stresses on the system during extreme events. The NASA Land Information System (LIS; Kumar et al. 2006; Peters-Lidard et al. 2007) runs operationally at the Short-term Prediction Research and Transition Center (Jedlovec 2013; Zavodsky et al. 2013; Case et al. 2016; <https://nasaspot.wordpress.com/category/land-information-system-lis/>) at NASA's Marshall Space Flight Center (Xia et al. 2012; Zhang et al. 2016; Vargas et al. 2015) to produce analyses and short-term forecasts of soil moisture and other fields. LIS is a land surface modeling and data assimilation framework designed to integrate satellite observations, including GPM and the Soil Moisture Active Passive (SMAP) satellite data (Entekhabi et al. 2010), into the modeling infrastructure (<http://lis.gsfc.nasa.gov/>). The integration of GPM data within LIS, run operationally at SPoRT, can capture soil moisture changes. For example, LIS identified an extreme soil moisture increase during the first week of October 2015, when a closed upper low over the southeastern United States combined with a deep tropical moisture plume associated with Hurricane Joaquin, resulting in historic rainfall over

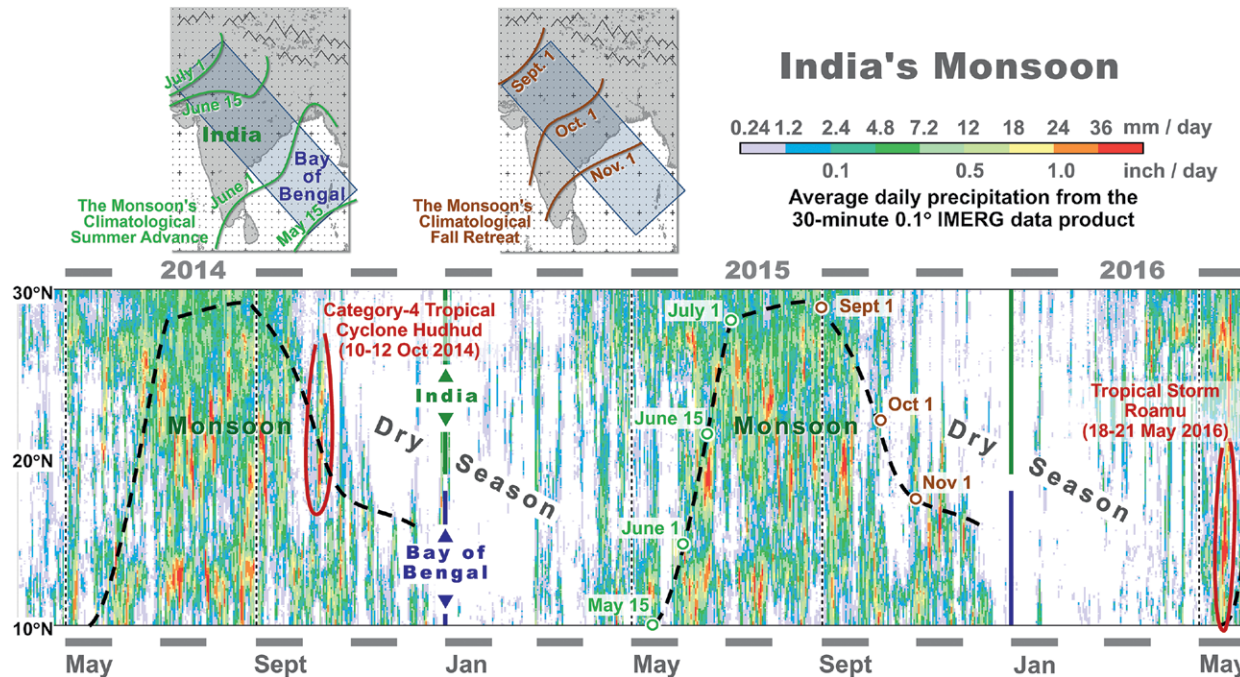


FIG. 9. GPM depicts characteristics of India's monsoons in 2014 and 2015. (bottom) The time–latitude plot summarizes the IMERG precipitation estimates over India from Apr 2014 through May 2016. The heavy black dashed line shows the climatological advance and retreat of India's monsoon. (top) The dates of the climatological advance and retreat are shown as well. The area over which IMERG was averaged is indicated by the blue-gray rectangle stretching across India and the Bay of Bengal; the latitude in (bottom) is along the midline of the rectangle, and the averages are taken along the perpendiculars to the midline.

the Carolinas. The SPoRT Center provided model outputs from LIS to Eastern Region NWS Forecast Offices in near-real time. In other cases, these data are also used by a variety of end users experimentally for assessing drought, flooding potential, and situational awareness for wildfire and blowing dust. There is great potential in the future for using GPM estimates together with other space-based soil moisture measurements from SMAP to improve weather and hydrological prediction.

The GPM suite of products contributes to a wide range of societal applications such as estimates of tropical cyclone location and intensity, famine early warning, drought monitoring, water resource management, agriculture, numerical weather prediction, land system modeling, global climate modeling, disease tracking, economic studies, and animal migration; many of which were initially developed with TRMM data. Many of these applications require near-real-time data as well as longer-term, well-calibrated precipitation information. IMERG is starting to be used as an input for forecasts in other regions of the world, especially areas lacking adequate ground-based coverage. Selected applications are reported upon in Kirschbaum et al. (2017), Ward et al. (2015), Kucera et al. (2013), and Kirschbaum and Patel (2016).

CONCLUSIONS AND NEXT STEPS. The Global Precipitation Measurement mission provides unprecedented and highly useful global precipitation datasets. GPM *Core Observatory* data are used to intercalibrate a set of precipitation observations from constellation partner sensors. By merging GPM multisatellite estimates with other IR satellite data, products with temporal resolutions down to 30 min and spatial resolutions as small as $0.1^\circ \times 0.1^\circ$ are possible. Latencies, at 1–5 h (depending on the product) after data collection, are vital for GPM's operational users. Research quality products (with accuracy requirements as indicated in the sidebar on GPM's mission science requirements) are available later (from 12 h to several months) for intensive scientific studies ranging from diagnosing microphysical precipitation particle characteristics to assessing regional and global patterns of precipitation. The GPM mission provides indispensable precipitation data from micro- to local to global scales via retrieved precipitation particle size distributions inside clouds, 5–15-km-resolution estimates of regional precipitation, and merged global precipitation.

GPM's algorithms have been updated several times (currently on version 05) with an additional update

planned for 2018–19. Current work is focused on reprocessing the level 0–3 products back to the beginning of TRMM (in 1998) and also for partner satellite datasets to establish a long and consistent record of precipitation. Scientific studies and societal applications using GPM data are ongoing and growing rapidly. Knowing the horizontal and vertical structures of precipitation is important for improving weather forecasting and climate change models. The planned processing of a consistent precipitation record encompassing the TRMM and GPM era will be of high value to future generations of scientific studies and user applications. The consistent TRMM-plus-GPM record will generate interesting scientific insights and reinvigorate applications in hydrological/land surface modeling and numerical weather prediction. Going forward in time, GPM's prime mission lifetime lasts until May 2017, at which time GPM will move into extended operations. Current predictions suggest that the station-keeping fuel will last 15 or more years, implying that instruments or spacecraft systems (like the batteries) will likely be the life-limiting factors as long as the fuel requirements do not increase.

In quantifying precipitation, a key Earth system component, the GPM mission provides fundamental knowledge of the water cycle and complements other NASA satellite missions, such as the Gravity Recovery and Climate Experiment (GRACE), which measures changes in groundwater levels in underground aquifers (among other observations) (Tapley et al. 2004); the Soil Moisture Active Passive (SMAP) satellite (Entekhabi et al. 2010); *Aquarius* (while it was operating), which observed ocean salinity (Le Vine et al. 2010); and *CloudSat*, which measures the properties of clouds and light precipitation (Stephens et al. 2002). Integrated multidisciplinary scientific investigations can provide greater understanding of our complex Earth system. GPM has and will continue to provide valuable and freely accessible precipitation data for science and society.

ACKNOWLEDGMENTS. This paper is dedicated to former GPM Project Scientist Arthur Y. Hou (1947–2013). Data are provided by NASA–JAXA. The climatological monsoon dates are from the Indian Meteorology Department. Imagery was generated by the NASA Goddard Space Flight Center, including the monsoon visualization by Owen Kelley. PMM Science Team members are acknowledged for their many contributions to GPM science. We thank our three anonymous reviewers for their thoughtful and paper-enhancing comments. Funding for this work was provided by NASA Headquarters (Grant NNH15ZDA001N-PMM), NOAA, and JAXA.

APPENDIX. List of key acronyms used in this paper.

3D	Three-dimensional	IR	Infrared
4D	Four-dimensional	ISRO	Indian Space Research Organization
AMSR-E2	Advanced Microwave Scanning Radiometer for Earth Observing System 2	JAXA	Japan Aerospace Exploration Agency
ASCII	American Standard Code for Information Exchange	JPSS-1	Joint Polar Satellite System-1
ATMS	Advanced Technology Microwave Sounder	JST	Japan standard time
CNES	Centre National d'Etudes Spatiales	LIS	Land Information System
CONUS	Continental United States	MAE	Mean absolute error
CORRA	Combined Radar–Radiometer Algorithm	MHS	Microwave Humidity Sounder
dBZ	Decibel relative to Z	MHz	Megahertz
DMSP	Defense Meteorological Satellite Program	MOS	Mission operations system
DPR	Dual-frequency Precipitation Radar	MRE	Mean relative error
EUMESAT	European Organisation for the Exploitation of Meteorological Satellites	MRMS	Multi-Radar/Multi-Sensor
FOV	Field of view	MSFC	Marshall Space Flight Center
GCOM-W1	<i>Global Change Observation Mission–Water</i>	NASA	National Aeronautics and Space Administration
GCPEX	Global Precipitation Measurement Cold Season Precipitation Experiment	NEDT	Noise-equivalent delta temperature
GHz	Gigahertz	NEXRAD	Next Generation Weather Radar
GIS	Geographic information system	NOAA	National Oceanic and Atmospheric Administration
GMI	GPM Microwave Imager	NPP	NASA Postdoctoral Program
GPCP	Global Precipitation Climatology Project	NRT	Near-real time
GPM	Global Precipitation Measurement	NS	Normal Scan algorithm
GPM CO	Global Precipitation Measurement <i>Core Observatory</i>	NWS	National Weather Service
GPROF	Goddard profiling algorithm	PMM	Precipitation Measurement Mission
GRACE	Gravity Recovery and Climate Experiment	PPS	Precipitation Processing System
GSFC	Goddard Space Flight Center	QPE	Quantitative precipitation estimate
GSMaP	Global Satellite Mapping of Precipitation	SAPHIR	Sounder for Probing Vertical Profiles of Humidity
GV	Ground validation	SMAP	Soil Moisture Active Passive
HDF5	Hierarchical data format	SPoRT	Short-term Prediction Research and Transition
IMERG	Integrated Multisatellite Retrievals for GPM	SSMIS	Special Sensor Microwave Imager/Sounder
		T_B	Brightness temperature
		TIFF	Tagged image file format
		TMI	TRMM Microwave Imager
		TRMM	Tropical Rainfall Measuring Mission
		U.S.	United States
		UTC	Coordinated universal time
		WMO	World Meteorological Organization
		WSR-88D	Weather Surveillance Radar-1988 Doppler

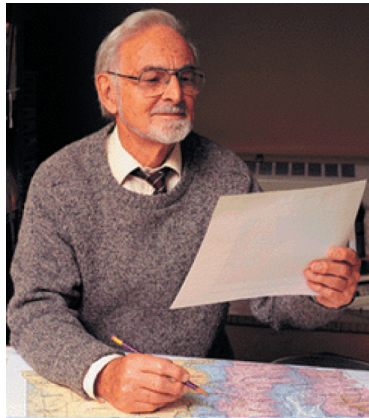
REFERENCES

- Adler, R. F., and Coauthors, 2003: The version-2 Global Precipitation Climatology Project (GPCP) monthly precipitation analysis (1979–present). *J. Hydrometeor.*, **4**, 1147–1167, doi:10.1175/1525-7541(2003)004<1147:TVGCP>2.0.CO;2.
- , J. J. Wang, G. Gu, and G. J. Huffman, 2009: A ten-year tropical rainfall climatology based on a composite of TRMM products. *J. Meteor. Soc. Japan*, **87**, 281–293, doi:10.2151/jmsj.87A.281.
- Aonashi, K., and Coauthors, 2009: GSMaP passive microwave precipitation retrieval algorithm: Algorithm description and validation. *J. Meteor. Soc. Japan*, **87A**, 119–136, doi:10.2151/jmsj.87A.119.
- Behrangi, A., G. Stephens, R. F. Adler, G. J. Huffman, B. Lambrightsen, and M. Lebsack, 2014: An update

- on the oceanic precipitation rate and its zonal distribution in light of advanced observations from space. *J. Climate*, **27**, 3957–3965, doi:10.1175/JCLI-D-13-00679.1.
- Berg, W., and Coauthors, 2016: Intercalibration of the GPM microwave radiometer constellation. *J. Atmos. Oceanic Technol.*, **33**, 2639–2654, doi:10.1175/JTECH-D-16-0100.1.
- Carr, N., and Coauthors, 2015: The influence of surface and precipitation characteristics on TRMM Microwave Imager rainfall retrieval uncertainty. *J. Hydrometeor.*, **16**, 1596–1614, doi:10.1175/JHM-D-14-0194.1.
- Case, J. L., K. D. White, B. Guyer, J. Meyer, J. Srikishen, C. B. Blankenship, and B. T. Zavodsky, 2016: Real-time Land Information System over the continental U.S. for situational awareness and local numerical weather prediction applications. *30th Conf. on Hydrology*, New Orleans, LA, Amer. Meteor. Soc., 3.3. [Available online at <https://ams.confex.com/ams/96Annual/webprogram/Paper287812.html>.]
- Chen, S., and Coauthors, 2013: Evaluation of spatial errors of precipitation rates and types from TRMM space-borne radar over the southern CONUS. *J. Hydrometeor.*, **14**, 1884–1896, doi:10.1175/JHM-D-13-027.1.
- Curtis, S., A. Salahuddin, R. F. Adler, G. J. Huffman, G. Gu, and Y. Hong, 2007: Precipitation extremes estimated by GPCP and TRMM: ENSO relationships. *J. Hydrometeor.*, **8**, 678–689, doi:10.1175/JHM601.1.
- Draper, D. W., D. A. Newell, D. A. Teusch, and P. K. Yoho, 2013: Global Precipitation Measurement Microwave Imager hot load calibration. *IEEE Trans. Geosci. Remote Sens.*, **51**, 4731–4742, doi:10.1109/TGRS.2013.2239300.
- , —, D. McKague, and J. Piepmeier, 2015a: Assessing calibration stability using the Global Precipitation Measurement (GPM) Microwave Imager (GMI) noise diodes. *IEEE J. Sel. Top. Geosci. Remote Sens.*, **8**, 4239–4247, doi:10.1109/JSTARS.2015.2406661.
- , —, F. J. Wentz, S. Krimchansky, and G. Skofronick-Jackson, 2015b: The Global Precipitation Measurement (GPM) Microwave Imager (GMI): Instrument overview and early on-orbit performance. *IEEE J. Sel. Top. Geosci. Remote Sens.*, **8**, 3452–3462, doi:10.1109/JSTARS.2015.2403303.
- Entekhabi, D., and Coauthors, 2010: The Soil Moisture Active Passive (SMAP) mission. *Proc. IEEE*, **98**, 704–716, doi:10.1109/JPROC.2010.2043918.
- Grecu, M., W. S. Olson, S. J. Munchak, S. Ringerud, L. Liao, Z. S. Haddad, B. L. Kelley, and S. F. McLaughlin, 2016: The GPM combined algorithm. *J. Atmos. Oceanic Technol.*, **33**, 2225–2245, doi:10.1175/JTECH-D-16-0019.1.
- Hou, A. Y., G. Skofronick-Jackson, C. Kummerow, and J. M. Shepherd, 2008: Global precipitation measurement. *Precipitation: Advances in Measurement, Estimation and Prediction*, S. Michaelides, Ed., Springer-Verlag, 131–169.
- , and Coauthors, 2013: NASA GPM Science Implementation Plan. NASA Goddard Space Flight Center, 162 pp. [Available online at <https://pmm.nasa.gov/resources/documents/gpm-science-implementation-plan>.]
- , and Coauthors, 2014: The Global Precipitation Measurement mission. *Bull. Amer. Meteor. Soc.*, **95**, 701–722, doi:10.1175/BAMS-D-13-00164.1.
- Houze, R. A., Jr., K. L. Rasmussen, M. D. Zuluaga, and S. R. Brodzik, 2015: The variable nature of convection in the tropics and subtropics: A legacy of 16 years of the Tropical Rainfall Measuring Mission satellite. *Rev. Geophys.*, **53**, 994–1021, doi:10.1002/2015RG000488.
- Huffman, G. J., D. T. Bolvin, D. Braithwaite, K. Hsu, R. Joyce, and P. Xie, 2015: NASA Global Precipitation Measurement (GPM) Integrated Multi-satellite Retrievals for GPM (I-MERG). Algorithm Theoretical Basis Doc. (ATBD), version 4.5, Greenbelt, MD, 26 pp. [Available online at http://pmm.nasa.gov/sites/default/files/document_files/IMERG_ATBD_V4.5.pdf.]
- Jedlovec, G., 2013: Transitioning research satellite data to the operational weather community: The SPoRT paradigm. *Geoscience and Remote Sensing Newsletter*, IEEE, New York, NY, 62–66, doi:10.1109/MGRS.2013.2244704.
- Kidd, C., A. Becker, G. J. Huffman, C. L. Muller, P. Joe, G. Skofronick-Jackson, D. B. Kirschbaum, 2017: So, how much of the Earth's surface is covered by rain gauges? *Bull. Amer. Meteor. Soc.*, **98**, 69–78, doi:10.1175/BAMS-D-14-00283.1.
- Kirschbaum, D. B., and K. Patel, 2016: Precipitation data key to food security and public health. *Eos, Trans. Amer. Geophys. Union*, **97**, doi:10.1029/2016EO045583.
- , and Coauthors, 2017: NASA's remotely sensed precipitation: A reservoir for applications users. *Bull. Amer. Meteor. Soc.*, **98**, 1169–1184, doi:10.1175/BAMS-D-15-00296.1.
- Kirstetter, P. E., and Coauthors, 2012: Toward a framework for systematic error modeling of spaceborne precipitation radar with NOAA/NSSL ground radar-based National Mosaic QPE. *J. Hydrometeor.*, **13**, 1285–1300, doi:10.1175/JHM-D-11-0139.1.
- , Y. Hong, J. J. Gourley, M. Schwaller, W. Petersen, and J. Zhang, 2013: Comparison of TRMM 2A25 products, version 6 and version 7, with NOAA/NSSL ground radar-based National Mosaic QPE. *J. Hydrometeor.*, **14**, 661–669, doi:10.1175/JHM-D-12-030.1.

- , Y. Hong, J. J. Gourley, Q. Cao, M. Schwaller, and W. Petersen, 2014: Research framework to bridge from the Global Precipitation Measurement mission core satellite to the constellation sensors using ground radar-based National Mosaic QPE. *Remote Sensing of the Terrestrial Water Cycle, Geophys. Monogr.*, Vol. 206, Amer. Geophys. Union, 61–79.
- , J. J. Gourley, Y. Hong, J. Zhang, S. Moazami-goodarzi, C. Langston, and A. Arthur, 2015a: Probabilistic precipitation rate estimates with ground-based radar networks. *Water Resour. Res.*, **51**, 1422–1442, doi:10.1002/2014WR015672.
- , Y. Hong, J. J. Gourley, M. Schwaller, W. Petersen, and Q. Cao, 2015b: Impact of sub-pixel rainfall variability on spaceborne precipitation estimation: Evaluating the TRMM 2A25 product. *Quart. J. Roy. Meteor. Soc.*, **141**, 953–966, doi:10.1002/qj.2416.
- Kojima, M., and Coauthors, 2012: Dual-frequency precipitation radar (DPR) development on the Global Precipitation Measurement (GPM) Core Observatory. *Earth Observing Missions and Sensors: Development, Implementation, and Characterization II*, H. Shimoda et al., Eds., International Society for Optical Engineering (SPIE Proceedings, Vol. 8528), 85281A, doi:10.1117/12.976823.
- Kozu, T., and Coauthors, 2001: Development of Precipitation Radar onboard the Tropical Rainfall Measuring Mission satellite. *IEEE Geosci. Remote Sens. Lett.*, **39**, 102–116, doi:10.1109/36.898669.
- Kubota, T., and Coauthors, 2007: Global precipitation map using satellite-borne microwave radiometers by the GSMAp project: Production and validation. *IEEE Trans. Geosci. Remote Sens.*, **45**, 2259–2275, doi:10.1109/TGRS.2007.895337.
- , and Coauthors, 2014: Evaluation of precipitation estimates by at-launch codes of GPM/DPR algorithms using synthetic data from TRMM/PR observations. *IEEE J. Sel. Top. Appl. Earth Obs. Remote Sens.*, **7**, 3931–3944, doi:10.1109/JSTARS.2014.2320960.
- , T. Iguchi, M. Kojima, L. Liao, T. Masaki, H. Harnado, R. Meneghini, and R. Oki, 2016: A statistical method for reducing sidelobe clutter for the Ku-band precipitation radar onboard the GPM Core Observatory. *J. Atmos. Oceanic Technol.*, **33**, 1413–1428, doi:10.1175/JTECH-D-15-0202.1.
- Kucera, P. A., E. E. Ebert, F. J. Turk, V. Levizzani, D. Kirschbaum, F. J. Tapiador, A. Loew, and M. Borsche, 2013: Precipitation from space: Advancing Earth system science. *Bull. Amer. Meteor. Soc.*, **94**, 365–375, doi:10.1175/BAMS-D-11-00171.1.
- Kumar, S. V., and Coauthors, 2006: Land information system: An interoperable framework for high resolution land surface modeling. *Environ. Modell. Software*, **21**, 1402–1415, doi:10.1016/j.envsoft.2005.07.004.
- Kummerow, C., W. Barnes, T. Kozu, J. Shiue, and J. Simpson, 1998: The Tropical Rainfall Measuring Mission (TRMM) sensor package. *J. Atmos. Oceanic Technol.*, **15**, 809–817, doi:10.1175/1520-0426(1998)015<0809:TTRMMT>2.0.CO;2.
- , and Coauthors, 2000: The status of the Tropical Rainfall Measuring Mission (TRMM) after two years in orbit. *J. Appl. Meteor.*, **39**, 1965–1982, doi:10.1175/1520-0450(2001)040<1965:TSOTTR>2.0.CO;2.
- , S. Ringerud, J. Crook, D. Randel, and W. Berg, 2011: An observationally generated a priori database for microwave rainfall retrievals. *J. Atmos. Oceanic Technol.*, **28**, 113–130, doi:10.1175/2010JTECHA1468.1.
- , D. L. Randel, M. Kulie, N.-Y. Wang, R. Ferraro, S. J. Munchak, and V. Petkovic, 2015: The evolution of the Goddard profiling algorithm to a fully parametric scheme. *J. Atmos. Oceanic Technol.*, **32**, 2265–2280, doi:10.1175/JTECH-D-15-0039.1.
- Le Vine, D. M., G. S. E. Lagerloef, and S. E. Torrusio, 2010: Aquarius and remote sensing of sea surface salinity from space. *Proc. IEEE*, **98**, 688–703, doi:10.1109/JPROC.2010.2040550.
- Liu, C., and E. J. Zipser, 2015: The global distribution of largest, deepest, and most intense precipitation systems. *Geophys. Res. Lett.*, **42**, 3591–3595, doi:10.1002/2015GL063776.
- , D. J. Cecil, E. J. Zipser, K. Kronfeld, and R. Robertson, 2012: Relationships between lightning flash rates and radar reflectivity vertical structures in thunderstorms over the tropics and subtropics. *J. Geophys. Res.*, **117**, D06212, doi:10.1029/2011JD017123.
- Liu, N., and C. Liu, 2016: Global distribution of deep convection reaching tropopause in 1 year GPM observations. *J. Geophys. Res. Atmos.*, **121**, 3824–3842, doi:10.1002/2015JD024430.
- Panegrossi, G., and Coauthors, 2016: Use of the GPM constellation for monitoring heavy precipitation events over the Mediterranean region. *IEEE J. Sel. Top. Appl. Earth Obs. Remote Sens.*, **9**, 2733–2753, doi:10.1109/JSTARS.2016.2520660.
- Peters-Lidard, C. D., and Coauthors, 2007: High-performance Earth system modeling with NASA/GSFC's Land Information System. *Innov. Syst. Softw. Eng.*, **3**, 157–165, doi:10.1007/s11334-007-0028-x.
- Prakash, S., A. K. Mitra, D. S. Pai, and A. AghaKouchak, 2016: From TRMM to GPM: How well can heavy rainfall be detected from space? *Adv. Water Resour.*, **88**, 1–7, doi:10.1016/j.advwatres.2015.11.008.
- Seto, S., T. Iguchi, T. Shimozuma, and S. Hayashi, 2015: NUBF correction methods for the GPM/DPR level-2 algorithms. *Int. Geoscience and Remote Sensing*

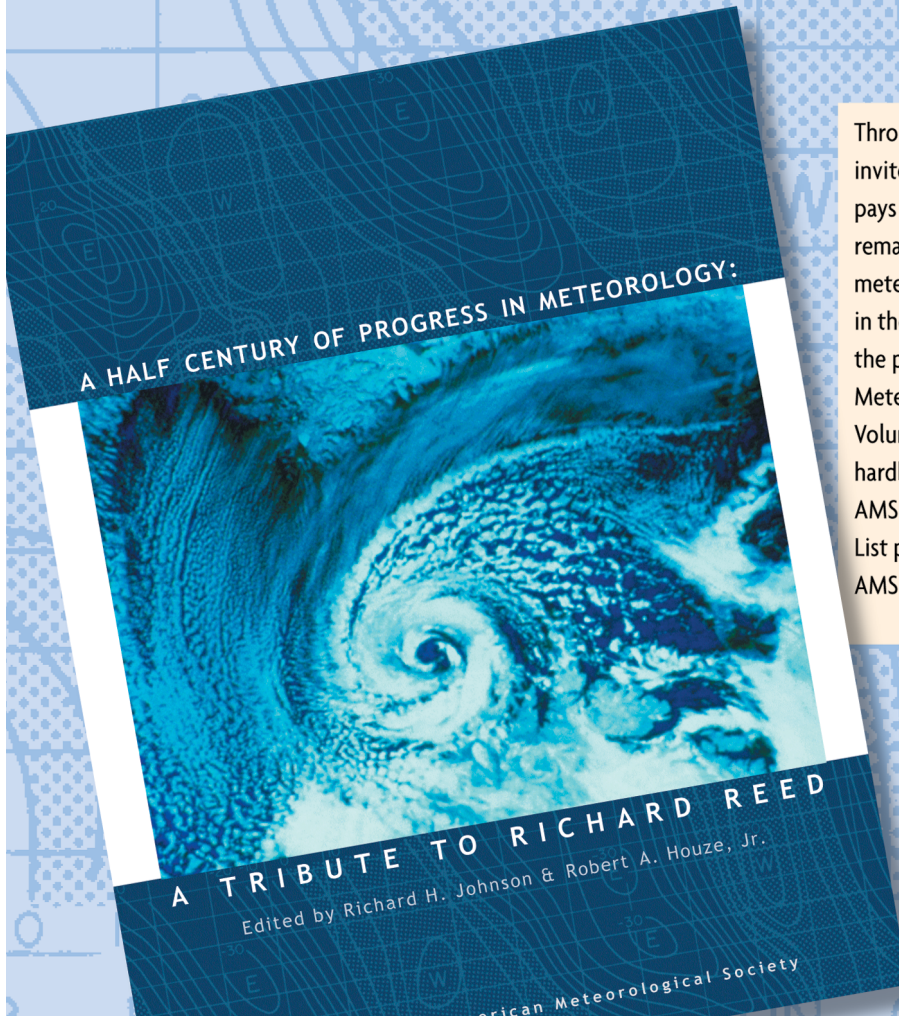
- Symp., Milan, Italy, IEEE, 2612–2614, doi:10.1109/IGARSS.2015.7326347.
- Shepherd, M., T. Mote, J. Dowd, M. Roden, P. Knox, S. C. McCutcheon, and S. E. Nelson, 2011: An overview of synoptic and mesoscale factors contributing to the disastrous Atlanta flood of 2009. *Bull. Amer. Meteor. Soc.*, **92**, 861–870, doi:10.1175/2010BAMS3003.1.
- Simpson, J. R., R. F. Adler, and G. R. North, 1988: A proposed Tropical Rainfall Measuring Mission (TRMM) satellite. *Bull. Amer. Meteor. Soc.*, **69**, 278–295, doi:10.1175/1520-0477(1988)069<0278:AP TRMM>2.0.CO;2.
- Skofronick-Jackson, and Coauthors, 2015: Global Precipitation Measurement Cold Season Precipitation Experiment (GCPEx): For measurement's sake let it snow. *Bull. Amer. Meteor. Soc.*, **96**, 1719–1741, doi:10.1175/BAMS-D-13-00262.1.
- Stephens, G. L., and Coauthors, 2002: The CloudSat mission and the A-Train: A new dimension of space-based observations of clouds and precipitation. *Bull. Amer. Meteor. Soc.*, **83**, 1771–1790, doi:10.1175/BAMS-83-12-1771.
- Tan, B.-Z., W. A. Petersen, and A. Tokay, 2016: A novel approach to identify sources of errors in IMERG for GPM ground validation. *J. Hydrometeor.*, **17**, 2477–2491, doi:10.1175/JHM-D-16-0079.1.
- , —, P. Kirstetter, and Y. Tian, 2017: Performance of IMERG as a function of spatiotemporal scale. *J. Hydrometeor.*, **18**, 307–319, doi:10.1175/JHM-D-16-0174.1.
- Tao, W.-K., and Coauthors, 2016: TRMM latent heating retrieval: Applications and comparisons with field campaigns and large-scale analyses. *Multiscale Convection-Coupled Systems in the Tropics, Meteor. Monogr.*, No. 56, Amer. Meteor. Soc., 2.1–2.34, doi:10.1175/AMSMONOGRAPH-D-15-0013.1.
- Tapley, B. D., S. Bettadpur, J. C. Ries, P. F. Thompson, and M. M. Watkins, 2004: GRACE measurements of mass variability in the Earth system. *Science*, **305**, 503–505, doi:10.1126/science.1099192.
- Toyoshima, K., H. Masunaga, and F. A. Furuzawa, 2015: Early evaluation of Ku- and Ka-band sensitivities for the Global Precipitation Measurement (GPM) Dual-Frequency Precipitation Radar (DPR). *SOLA*, **11**, 14–17, doi:10.2151/sola.2015-004.
- Ushio, T., and Coauthors, 2009: A Kalman filter approach to the Global Satellite Mapping of Precipitation (GSMaP) from combined passive microwave and infrared radiometric data. *J. Meteor. Soc. Japan*, **87A**, 137–151, doi:10.2151/jmsj.87A.137.
- Vargas, M., Z. Jiang, J. Ju, and I. A. Csiszar, 2015: Real-time daily rolling weekly green vegetation fraction (GVF) derived from the Visible Imaging Radiometer Suite (VIIRS) sensor onboard the SNPP satellite. *20th Conf. Satellite Meteorology and Oceanography*, Phoenix, AZ, Amer. Meteor. Soc., P210. [Available online at <https://ams.confex.com/ams/95Annual/webprogram/Paper259494.html>.]
- Ward, A., D. Kirschbaum, and M. Hobish, 2015: Measuring rain and snow for science and society: The Second GPM Applications Workshop. *Earth Observer*, Vol. 27, No. 5, NASA GSFC, Greenbelt, MD, 4–11. [Available online at http://eospso.nasa.gov/sites/default/files/eo_pdfs/Sep_Oct_2015_color_508.pdf#page=4.]
- Wentz, F. J. and D. Draper, 2016: On-orbit absolute calibration of the Global Precipitation Measurement Microwave Imager. *J. Atmos. Oceanic Technol.*, **33**, 1393–1412, doi:10.1175/JTECH-D-15-0212.1.
- , and T. Meissner, 2016: Atmospheric absorption model for dry air and water vapor at microwave frequencies below 100 GHz derived from spaceborne radiometer observations. *Radio Sci.*, **51**, 381–391, doi:10.1002/2015RS005858.
- Wilheit, T., 2013: Comparing calibrations of similar conically scanning window-channel microwave radiometers. *IEEE Trans. Geosci. Remote Sens.*, **51**, 1453–1464, doi:10.1109/TGRS.2012.2207122.
- , W. Berg, H. Ebromami, R. Kroodsma, D. McKague, V. Payne, and J. Wang, 2015: Intercalibrating the GPM constellation using the GPM microwave imager (GMI). *Int. Geoscience and Remote Sensing Symp.*, Milan, Italy, IEEE, 5162–5165, doi:10.1109/IGARSS.2015.7326996.
- Xia, Y., and Coauthors, 2012: Continental-scale water and energy flux analysis and validation for the North American Land Data Assimilation System project phase 2 (NLDAS-2): 1. Intercomparison and application of model products. *J. Geophys. Res.*, **117**, D03109, doi:10.1029/2011JD016048.
- Zavodsky, B. T., J. L. Case, C. B. Blankenship, W. L. Crosson, and K. D. White, 2013: Application of next-generation satellite data to a high-resolution, real-time land surface model. *Earthzine*, IEEE, New York, NY. [Available online at www.earthzine.org/2013/04/10/application-of-next-generation-satellite-data-to-a-high-resolution-real-time-land-surface-model/.]
- Zhang, J., and Coauthors, 2011: National Mosaic and Multi-sensor QPE (NMQ) system: Description, results, and future plans. *Bull. Amer. Meteor. Soc.*, **92**, 1321–1338, doi:10.1175/2011BAMS-D-11-00047.1.
- , and Coauthors, 2016: Multi-Radar Multi-Sensor (MRMS) quantitative precipitation estimation: Initial operating capabilities. *Bull. Amer. Meteor. Soc.*, **97**, 621–638, doi:10.1175/BAMS-D-14-00174.1.



A Half Century of Progress in Meteorology: A Tribute to Richard Reed

edited by Richard H. Johnson and Robert A. Houze Jr.

with selections by: Lance F. Bosart Robert W. Burpee Anthony Hollingsworth
James R. Holton Brian J. Hoskins Richard S. Lindzen John S. Perry Erik A. Rasmussen
Adrian Simmons Pedro Viterbo



Through a series of reviews by invited experts, this monograph pays tribute to Richard Reed's remarkable contributions to meteorology and his leadership in the science community over the past 50 years. 2003.

Meteorological Monograph Series,
Volume 31, Number 53; 139 pages,
hardbound; ISBN 1-878220-58-6;
AMS Code MM53.

List price: \$80.00

AMS Member price: \$60.00

ORDER ONLINE: bookstore.ametsoc.org or see the order form at the back of this issue